The study on the dynamic response of cylindrical pressure hull on the different shock loading empirical formula

Ching-Yu Hsu[1,a], Tso-Liang Teng[2,b],
Cho-Chung Liang[3,c] , Hai-Anh Nguyen[2,d] and Chien-Jong Shih [4,e]

[1]Department of Marine Mechanical Engineering , ROC Naval Academy, Taiwan

[2]Hsiuping University of Science and Technology, Taichung, Taiwan

[3]Department of Mechanical and Automation Engineering, Da-Yeh University, Changhua, Taiwan

Department of Mechanical and Electro-Mechanical Engineering, Tam-Kang University, Taipei, Tawan

[a]cyhsu@mail.cna.edu.tw, [b]tlteng@mail.hust.edu.tw, [c]ccliang@mail.dyu.edu.tw,
[d]h2k1990@gmail.com, [e]cjs@mail.tku.edu.tw

Keywords: Underwater Explosion, UNDEX Loading Empirical Formula, Shockwave

Abstract. This paper focuses on the comparison between underwater explosion (UNDEX) shock loading empirical formulations. First, the numerical simulations for a cylindrical pressure hull subjected to UNDEX loading were conducted and the results are close to the failure modes shown in experiments of Kwon (1993). Second, the empirical UNDEX loading formula of Cole (1948), Keil (1961) and Shin (1994) used in cylinder subjected to underwater shock loading were compared. The simulation results by using three empirical formulas were compared and Shin's (or Cole's) empirical formula was shown to be better than the other empirical formulations when subjected to an UNDEX under the same conditions. The analytical results offer a valuable reference to the research of underwater explosion.

Introduction

In recent years, there has been considerable interest in evaluating the role of predicting how submerged structures are damaged by UNDEX. In particular, cylindrical shell structures are crucial components of submerged ships and marine structures. Numerical methods for analyzing submerged structures exposed to UNDEX shock loadings have been successfully implemented. For example, Kwon [1] simulated the nonlinear dynamic response of a cylinder subjected to a side-on shock wave by using both numerical simulation and experimental (1993). Ramajeyathilagam [2] used a box model set-up under a shock tank and explosive charges of PEK-I to perform numerical investigations on thin rectangular plates subjected to UNDEX loading with the CSA/GENSA software (2004). Shin [3] presented ship shock modeling and simulation for far-field underwater explosion by applying the LS-DYNA code coupled with USA code (2004). Liang [4] studied a preliminary study of the transient responses of a 2000-ton patrol boat with shock loading using the finite element method (FEM) coupled with the second Doubly Asymptotic Approximation (DAA2) (2006). Wang [5] examined the dynamic response of ship structures with the combined effect of shock wave load and bubble pulsation subjected to close-in non-contact UNDEX (2014). Chen [6] conducted a numerical study of protective effect of polymer coating on the circular steel plate response to near-field underwater explosion (2015).

This paper applied acoustic-structure coupling (ASC) method used in ABAQUS and empirical formulation to simulate an UNDEX and investigate which is the best empirical formula. Three empirical formulas are selected to simulate the experiment of Kwon [1] are Shin [7], Cole [8] and Keil [9]. In the aforementioned literature the UNDEX response studied a lot of empirical formulation and the unit is not unity; however, no studies have shown what is the best empirical formula for simulating UNDEX. For that reason, comparing dynamic response of a cylindrical with the difference empirical fomula is the main issue of this research.

Numerical method

Empirical Formula for Shockwave. An explosion is a chemical reaction that converts the initial material into a gas at an extremely high temperature and pressure; the process occurs with extreme rapidity and emits a substantial amount of heat. The temperature in the product gases is approximately 3000^{o}C and the pressure is 50000 atm. Empirical equations were determined to define the profile of the shock wave and can be expressed as follows [7]:

$$P_{\max} = K_1 \left(\frac{W^{1/3}}{R} \right)^{A_1} \quad (1) \qquad \lambda = K_2 W^{1/3} \left(\frac{W^{1/3}}{R} \right)^{A_2} \quad (2) \qquad P(t) = P_{max} e^{-t/\lambda} \quad (3)$$

*K1, A1, K2 and A2 are c*onstants depending on various explosive charge types, listed in Table 1.

Other variables in the equations are:

W : the weight of the explosive charge (Kg); R: the distance between explosive charge and target (m)

$P(t)$: the pressure profile of the shock wave (MPa); P_{max}: the peak of the pressure of the wave. (MPa)

λ :the shock wave decay constant. (millisecond, ms)

Acoustic-structure coupling method. In the numerical simulation of interaction between shock wave and structure, the acoustic structural coupling method used in ABAQUS software is applied [10]. Acoustic element is introduced into the flow field, and its size is selected according to literature [10], as the model shown in Figure 1. The main principle and theoretical formula of acoustic-structural coupling method can refer to the theory of ABAQUS software manual [10].

Acoustic fields are strongly dependent on the conditions at the boundary of the acoustic medium. The boundary of a region of acoustic medium can be divided into sub regions S. Consider a surface cylinder floating on the free surface, as shown in Figure 1 The boundaries of this model are: S_{fp} where the value of the acoustic pressure p is prescribed; S_{ft} where we prescribe the normal derivative of the acoustic medium; S_{fr} the "reactive" acoustic boundary, where there is a prescribed linear relationship between the fluid acoustic pressure and its normal derivative; S_{fi} the "radiating" acoustic boundary; S_{fs} ,where the motion of an acoustic medium is directly coupled to the motion of a solid; S_{frs} ,an acoustic-structural boundary, where the displacements are linearly coupled but not necessarily identically equal due to the presence of a compliant or reactive intervening layer; S_{ft}, a boundary between acoustic fluids of possibly differing material properties [10].

Validation

This example problem is based upon an UNDEX experiment in which a submerged test cylinder is exposed to a pressure shock wave produced by a 60lb (27.3Kg) HBX-1 explosive charge. Kwon and Fox [1] originally described the experiment along with a set of selected experimental results.

The test cylinder was made of T6061-T6 aluminum (engineering properties of the material are given in Table 2). It had an overall length of 1.067m, an outside diameter of 0.305m, a wall thickness of 6.35 mm, and 24.5-mm-thick welded end plates. The cylinder was suspended horizontally in a 40-m-deep fresh water test quarry. The 27.3-kg HBX-I explosive charge and the cylinder were placed at a depth of 3.66 m. The charge was centered at the side of the cylinder and located 7.62 m from the cylinder surface. The suspension depths, charge offset, and duration of the test were selected such that cavitation of the fluid was not substantial and no bubble pulse occurred. Strain gauges were placed in multiple locations on the outer surface of the test cylinder, as shown in Figure 2.

Two pressure sensors were positioned 7.62 m from the charge; they were away from the cylinder, but were at the same depth as it. These sensors provided an experimental determination for the pressure versus time history of the spherical incident shock wave as it traveled by the point on the cylinder closest to the charge (strain gauge location B1). Figure 3 shows a time history curve of the incident pressure wave recorded by the sensors and empirical formula [7] from (1) and (2). As shown in the graphs, from 0 s to 0.0002 s, the pressure according to the experimental data [1] and the pressure according to Shin's formula were generated by a charge of 15.7MPa and 16.8MPa, respectively.

Between 0.0002 s and 0.002 s the higher value belonged to the experimental data. The rest remained unchanged (approximately 0).
Figure 4 (a) shows that the test cylinder was meshed with 2400 S4R finite strain shell elements and contained 2402 nodes, 2400 elements with 40 circumferential divisions, and 53 axial divisions. The external fluid was meshed with 4-node that consisted of 8923 nodes and 45586 elements. AC3D4 acoustic tetrahedral elements are shown in Figure 4 (b). The outer boundary of the external fluid is represented by a cylindrical surface with spherical ends. The characteristic radius of the fluid outer boundary is equal to 0.915m. Figure 4 (c) shows the profile of the cylinder and external fluid models. Fig.5 to Fig.10 contain time history plots of the test cylinder strains obtained from the ABAQUS analysis, with experimental shock loading data for locations of the strain measurements provided in Figure 4. The experimental data was digitized from a published curve [1]. Axial and hoop strains obtained from experimental and numerical analyses were consistent, as shown in the figures (Figure 5-10). The numerical response had the same shape as the experimental results (the numerical response according to Shin's empirical formula and the numerical response according to the experimental data [1] inputted into ABAQUS were identical). In addition, the results used for Shin's formula as shock loading input improved slightly compared with those used for the experimental value [10]. However, several variations existed when comparing data between the numerical results and experimental data [1]. The data matched the experimental results closely at B1 and B2, but less closely at position A,C (except for axial strain of C1). Numerical and experimental results matched more closely in areas with lower values of strain. Less oscillation of hoop strains at experimental and numerical solutions were shown compared with axial strains. The numerical method adopted in the simulations was sufficiently accurate in terms of the complex UNDEX process.

The dynamic response of cylindrical pressure hull on the different shock loading empirical formula

In this section, we apply the above method and simulation to compare the empirical formulation of Shin [7], Cole [8] and Keil [9]. There are many types of explosives such as TNT, HBX-1, PETN, Nuclear..etc.. To simplify, in this study, we only compare the empirical formula for the coefficient of TNT explosives (Table 3).
Using the validated method in Section 3, the numerical strain response of each location on cylinder are shown in Figure 11 to Figure 16. The response curves are very close both magnitude and phasing (The curve of Shin's empirical formula and Cole's empirical formula were identical). The results used for Shin's formula (or Cole) as shock loading input improved slightly compared with Keil's formula. The comparison here valuable in some cases is choosing the most appropriate formula. For example, on the structural design requirements high safety factor so Shin's empirical formula should be chosen to study

Conclusion

Numerical simulations of a cylinder model subjected to underwater shock wave loading were conducted in this study, and a procedure to analyze and compare the dynamic response of cylindrical by using the different empirical formula was developed. This study showed that the FEM, Shin's formulas, and acoustic-structure coupling method were effective tools for identifying the response of the structure subjected to UNDEX analysis. The results indicated that with the same UNDEX conditions, the empirical formula of Shin (or Cole) was better than the other formulation, and can be applied quantitatively to real structural design.

Acknowledgements

The authors would like to acknowledge the Ministry of Science and Technology of R.O.C for financially supporting this work under contract MOST 103-2221-E-212-018-MY3.

References

[1] Kwon, Y. W., Fox, P. K., Underwater shock responses of a cylinder subjected to aside-on explosion. Comput. Struct., 48 (4), 1993：646–737.

[2] Ramajeyathilagam K, Vendhan CP. Deformation and rupture of thin rectangular plates subjected to underwater shock. International Journal of Impact Engineering 2004;30(6): 699-719.

[3] Shin YS. Ship shock modeling and simulation for far-field underwater explosion. Computers & Structures 2004;82:2211-2219.

[4] Liang CC, Tai YS. Shock response of a surface ship subjected to noncontact underwater explosions. Ocean Engineering 2006; 33:748-772.

[5] Wang H, Zhu X, Cheng YS, Lin J. Experimental and numerical investigation of ship structure subjected to close-in underwater shock wave and following gas bubble pulse . Marine Structures 2014; 39:90–117.

[6] Chen Y, Chen F, Du ZP, Wang Y, Zhao PD, Hua HX. Protective effect of polymer coating on the circular steel plate response to near-field underwater explosion. Marine Structures 2015;40:247-266.

[7] Shin, Y.S, Naval Ship Shock Design and Analysis. Short Course Presented at Chung Cheng Institute of Technology, Aug., 1994.

[8] Cole, R. H., Underwater Explosion. Princeton University Press, New York, 1948

[9] Keil, A. H., The Response of Ships to Underwater Explosion. paper7, The Annual Meeting of the Society of Naval Architect and Marine Engineering, New York, 1961：366-410m.

[10] ABAQUS user's and theory manuals, version 6.11.1 Dassault Systèmes, RI, USA, 2011.

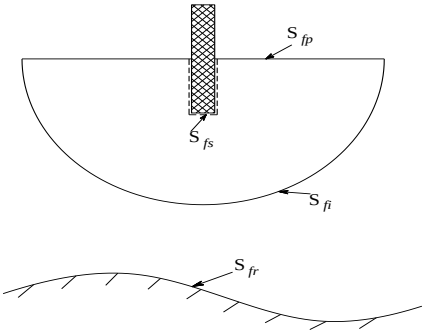

Figure 1 Fluid domain and boundaries

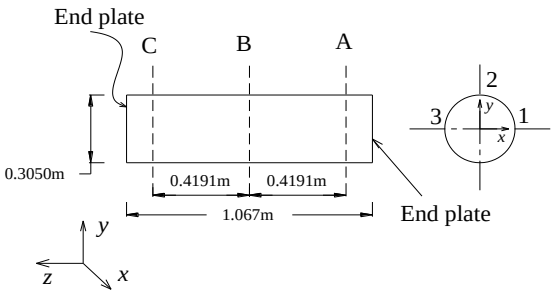

Figure 2 Strain gauge locations
(A1,A2, B1, B2, B3, C1, C2)with B1 closest to the charge

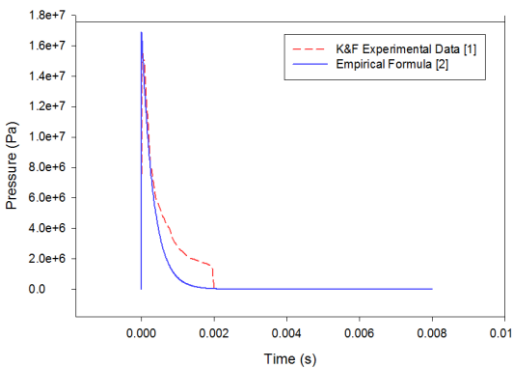

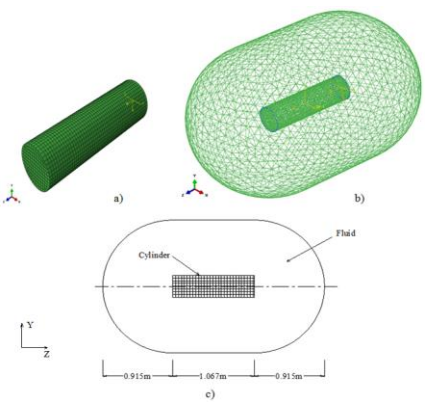

Figure 3: Incident pressure wave transient (shock pulse)

Figure 4: Test cylinder model and external fluid model

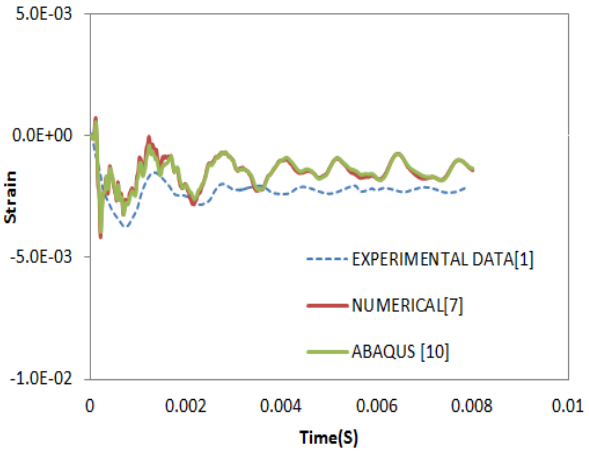

Figure 5 Experimental and numerical comparison for position A1(axial strain)

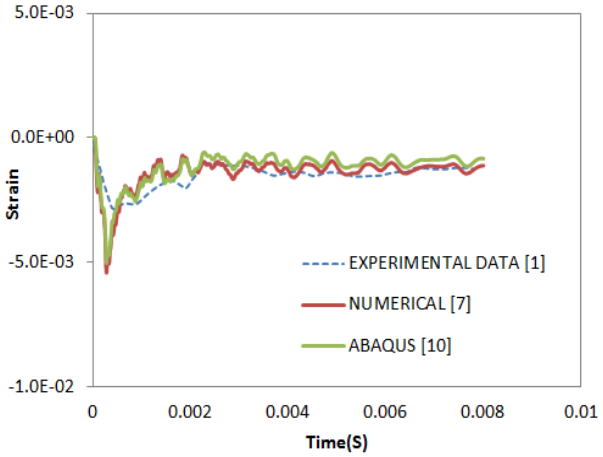

Figure 6 Experimental and numerical comparison for position A2(hoop strain)

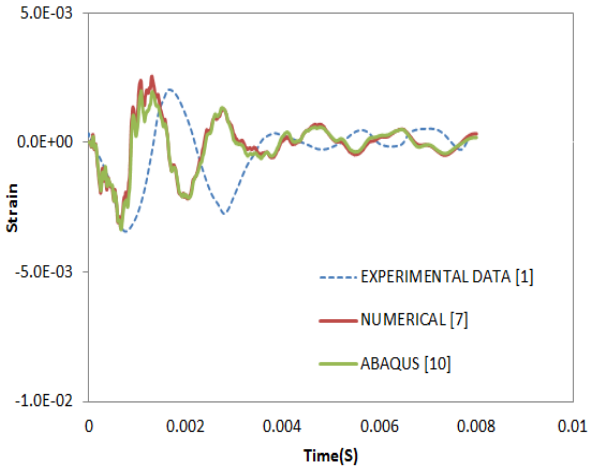

Figure 7 Experimental and numerical comparison for position B1(axial strain)

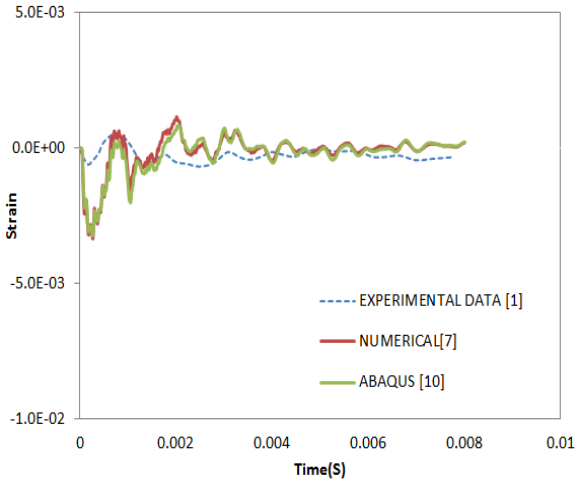

Figure 8 Experimental and numerical comparison for position B2(hoop strain)

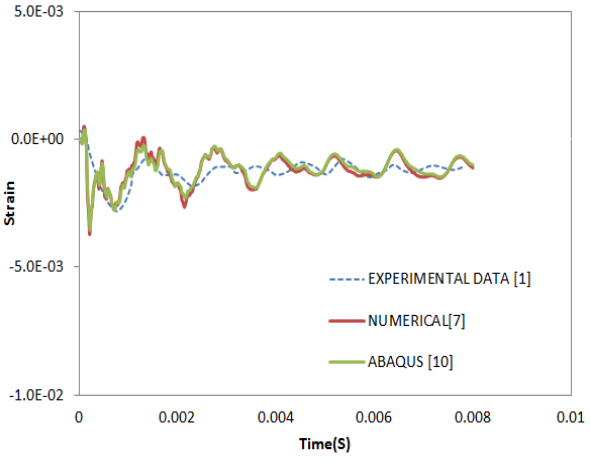

Figure 9 Experimental and numerical comparison for position C1(axial strain)

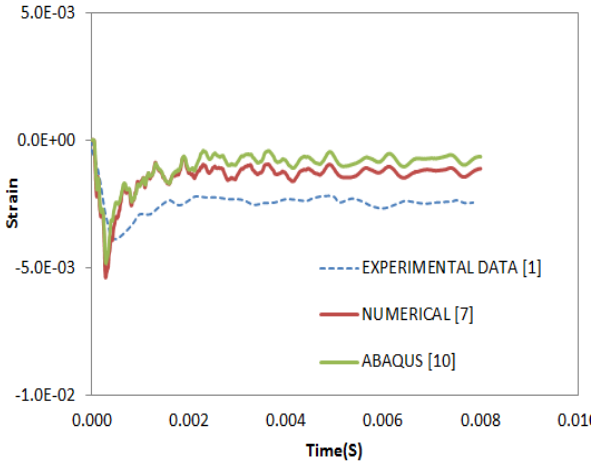

Figure 10 Experimental and numerical comparison for position C2(hoop strain)

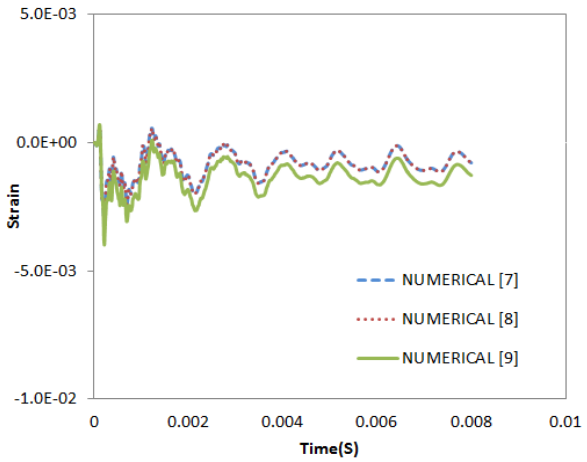

Figure 11 Numerical comparison for position A1(axial strain

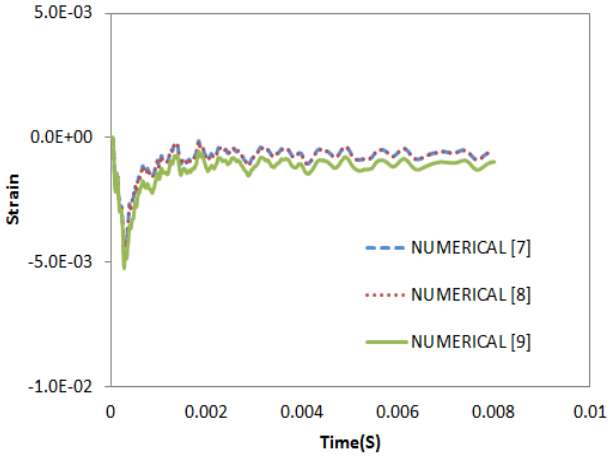

Figure 12 Numerical comparison for position A2(hoop strain)

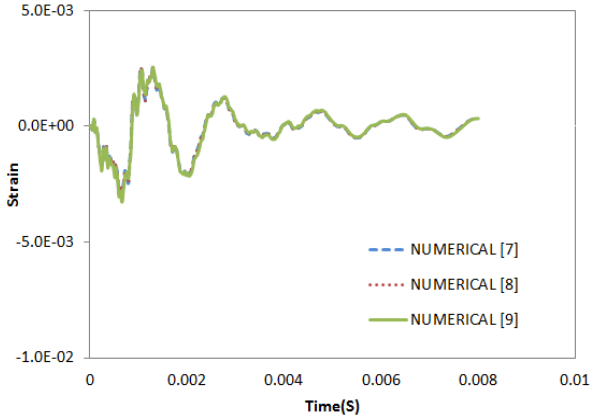

Figure 13 Numerical comparison for position B1(axial strain)

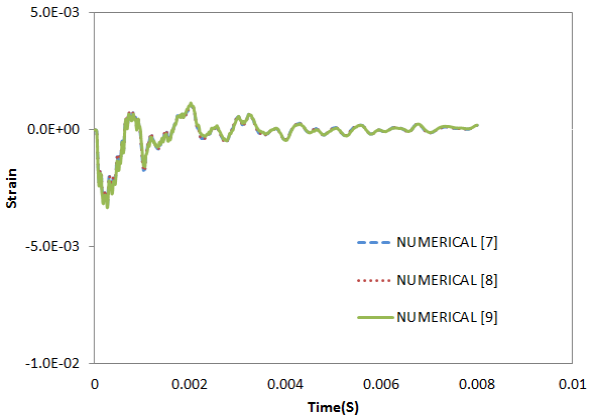

Figure 14: Numerical comparison for position B2(hoop strain)

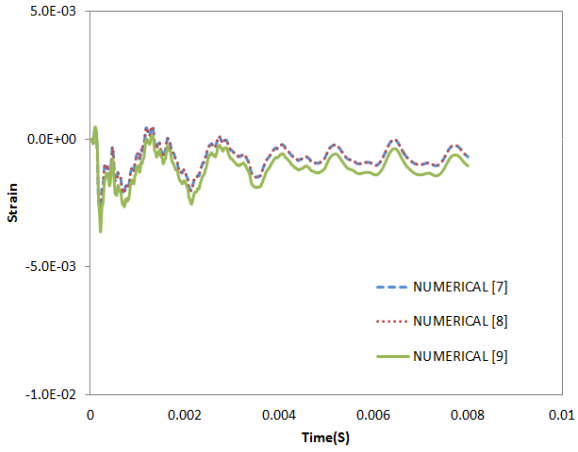

Figure 15 Numerical comparison for position C1(axial strain)

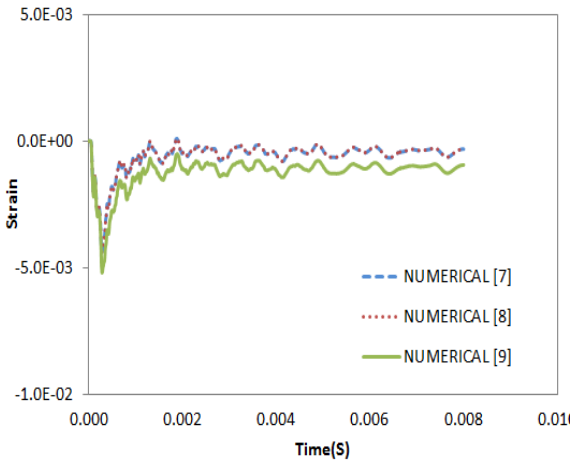

Figure 16 Numerical comparison for position C2(hoop strain).

Table 1: Shock wave constants

	HBX-1	TNT	PETN	Nuclear
K1	53.44	52.2	53.59	1.07×10^{4}
A1	1.144	1.18	1.194	1.13
K2	0.092	0.0894	0.086	3.627
A2	-0.247	-0.185	-0.257	-0.22

Table 2: Engineering properties of the material

Property	Value
Young's modulus (MPa)	75.6×103
Poisson's ratio	0.33
Mass density (Kg/m3)	2784
Static yield stress (MPa)	300

Table 3: Empirical Formulation

Description (TNT)	Shin[7]	Cole[8]	Keil[9]
K1	52.2	52.12	53.01
A1	1.18	1.18	1.13
K2	0.0894	0.0895	0.092
A2	-0.185	-0.185	-0.22